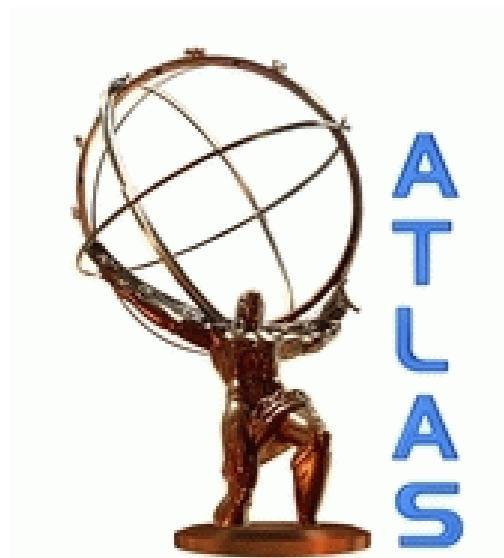
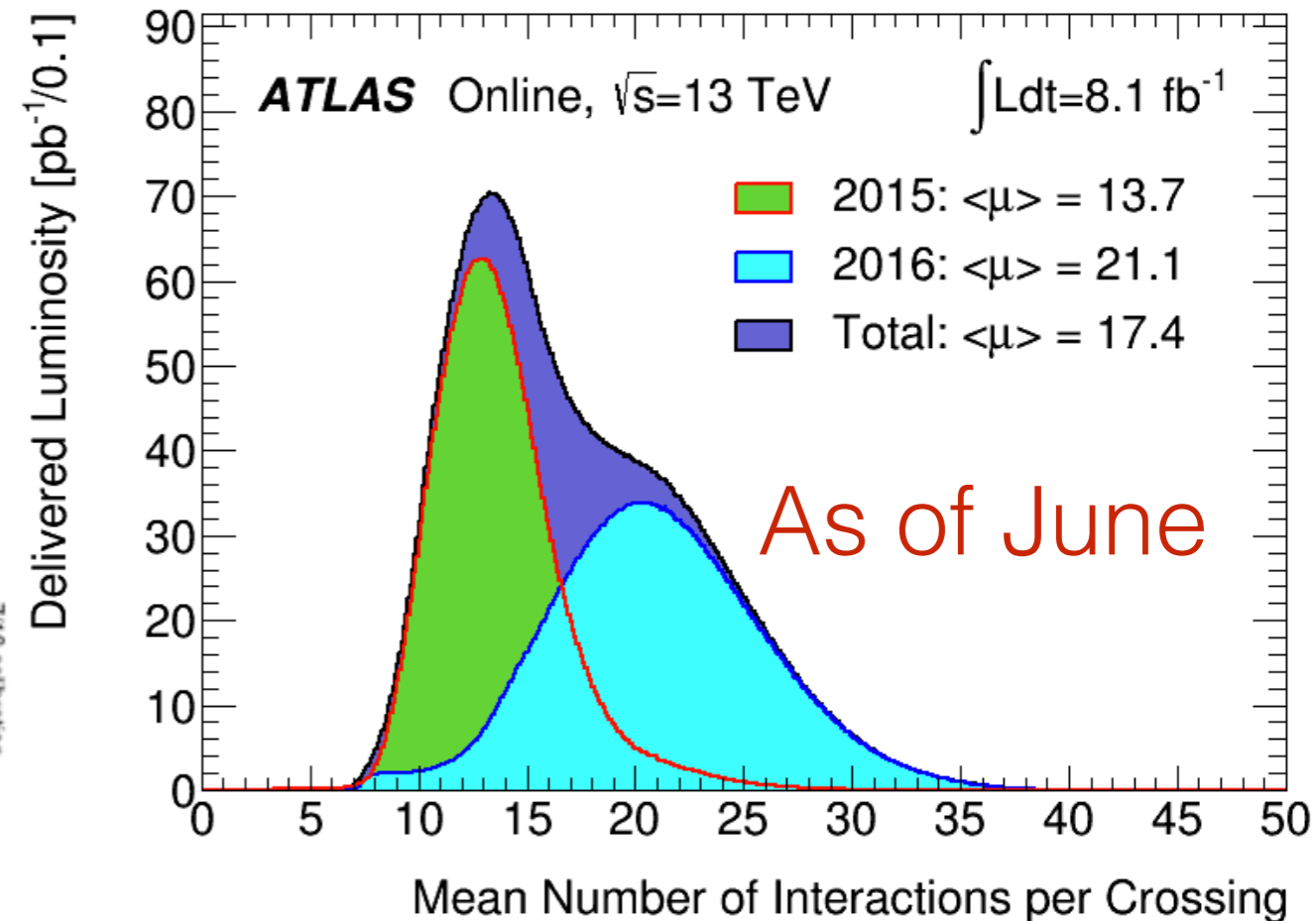
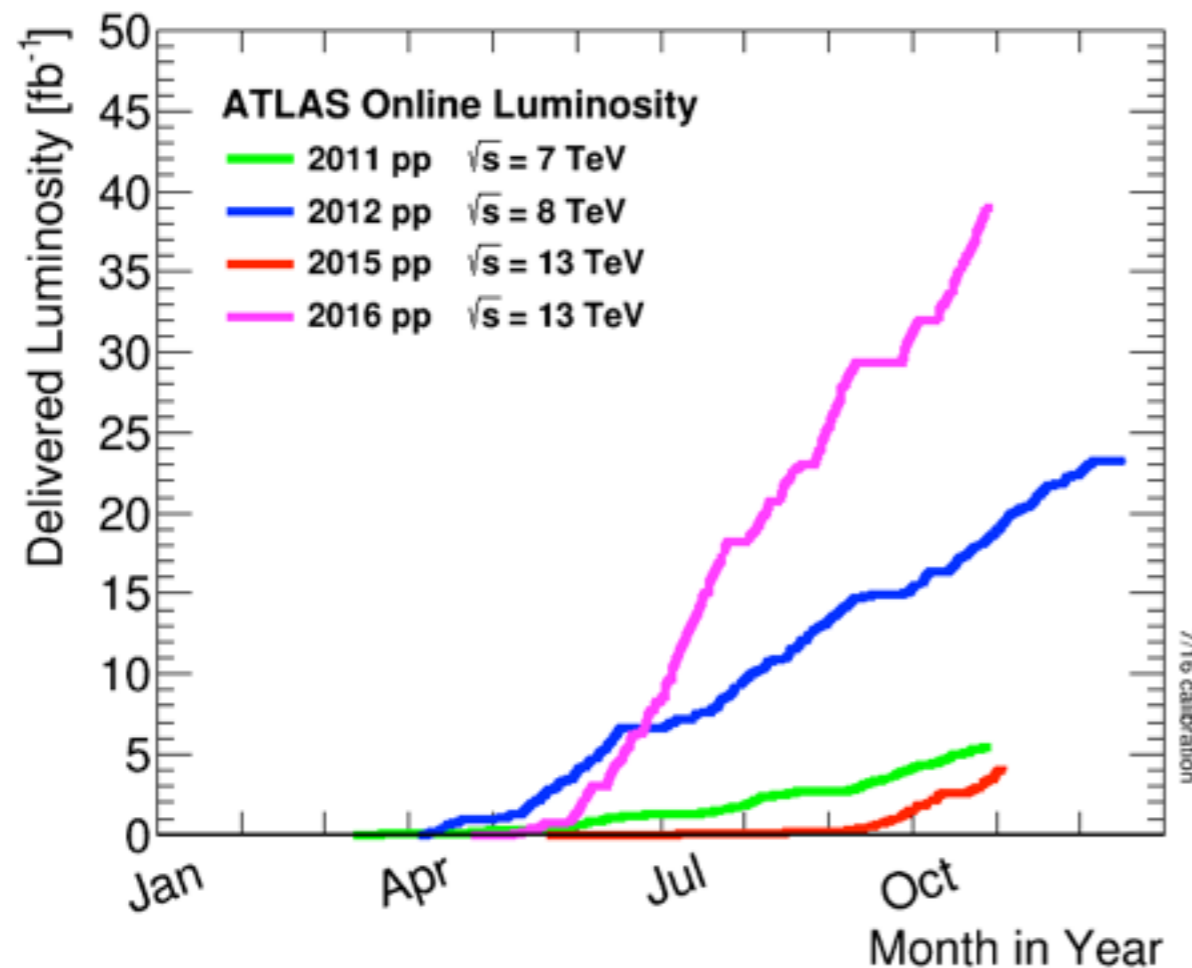


Measurement of the properties of the Higgs Boson in 13 TeV ATLAS data in the $H \rightarrow 4\ell$ decay channel

Will Leight
November 22, 2016

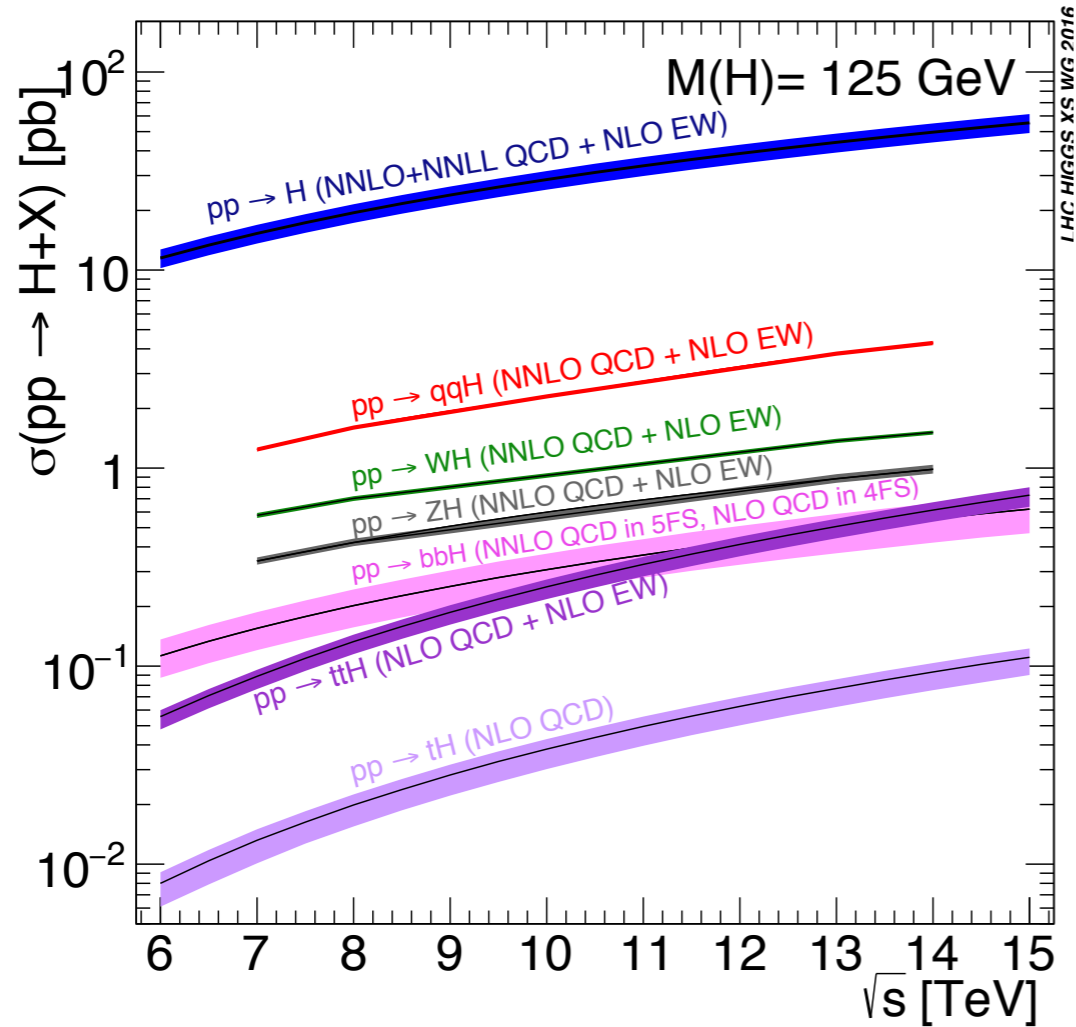


The LHC in Run-2



- Excellent performance by the LHC this year.
- The results shown here represent 13.3-14.8 fb⁻¹ of data at 13 TeV recorded in 2015 and 2016.
 - Our sensitivity to the Higgs is now higher than it was in Run-1.

Higgs Boson Production

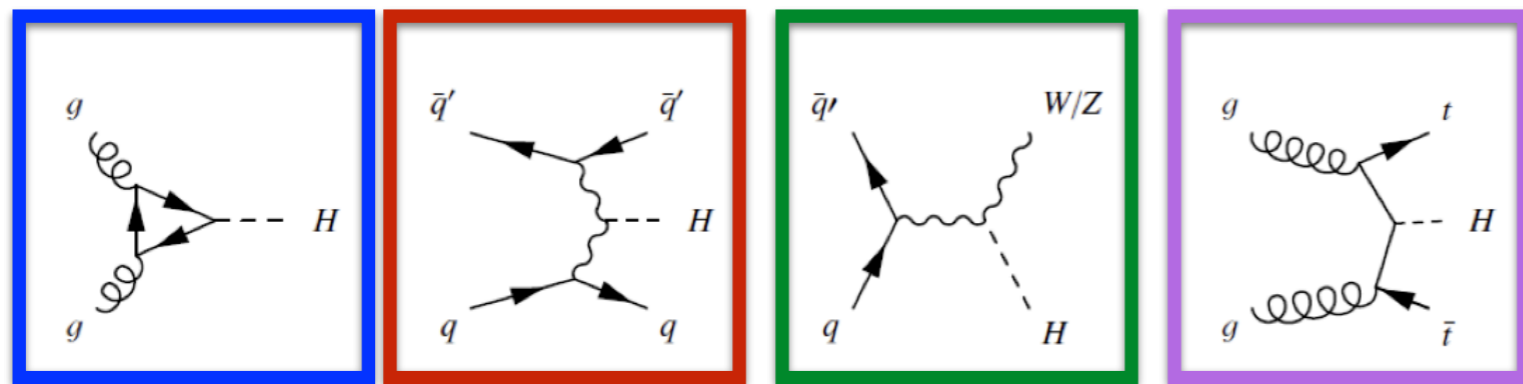


LHC Higgs XS WG

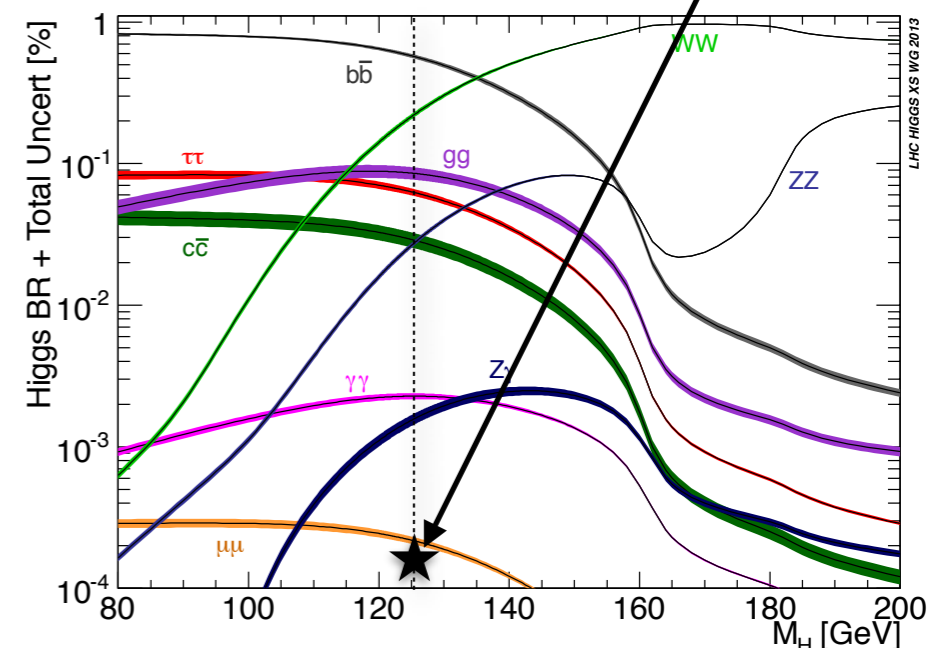
ggF	87.2%
VBF	6.8%
VH	4.1%
bbH/ttH/tH	1.9%

arxiv 1101.0593

$H \rightarrow ZZ \rightarrow 4\ell$ BR ~ .013%

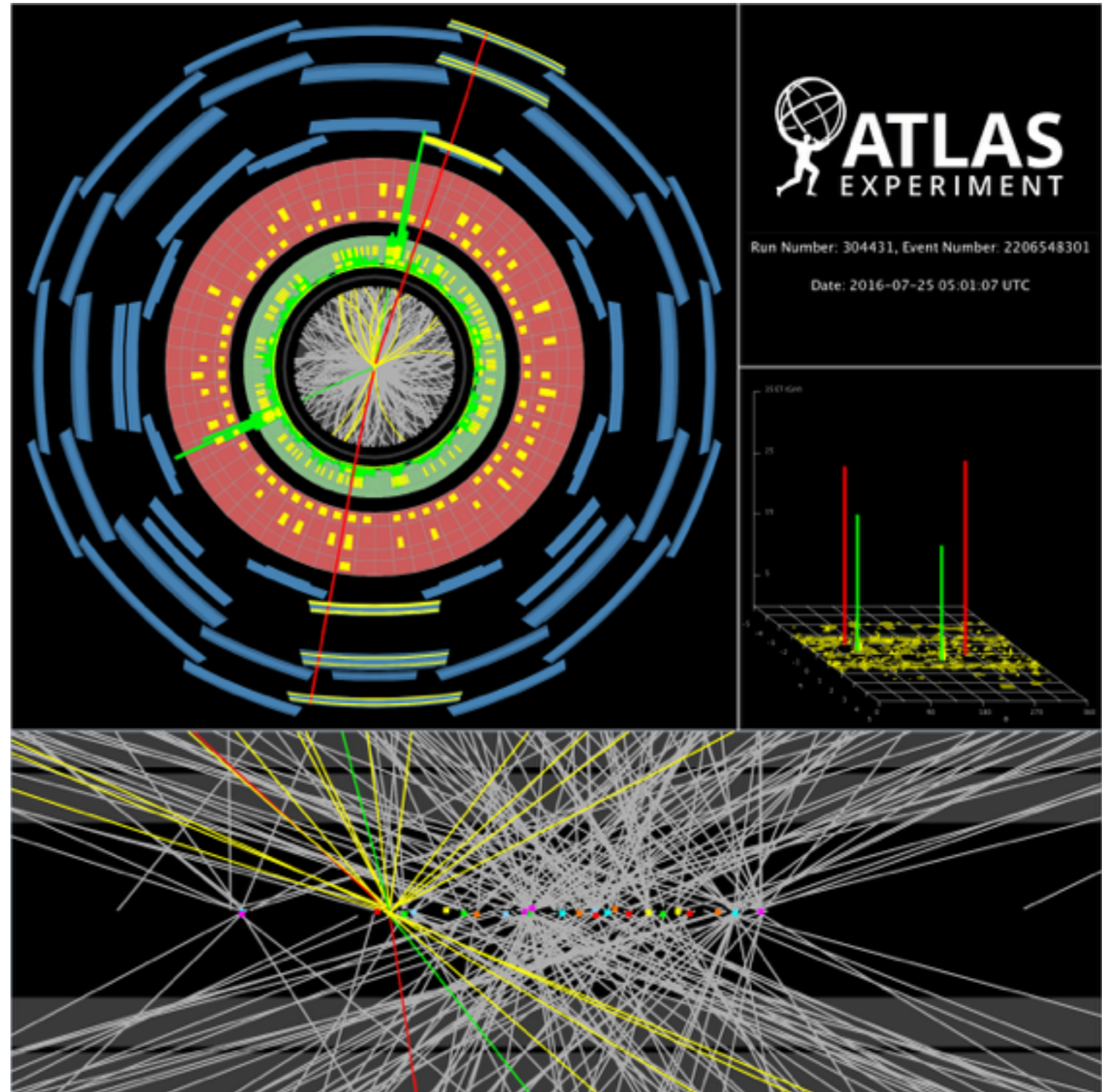


$$\sigma_{\text{tot}}(13 \text{ TeV}) \sim 2\sigma_{\text{tot}}(8 \text{ TeV})$$

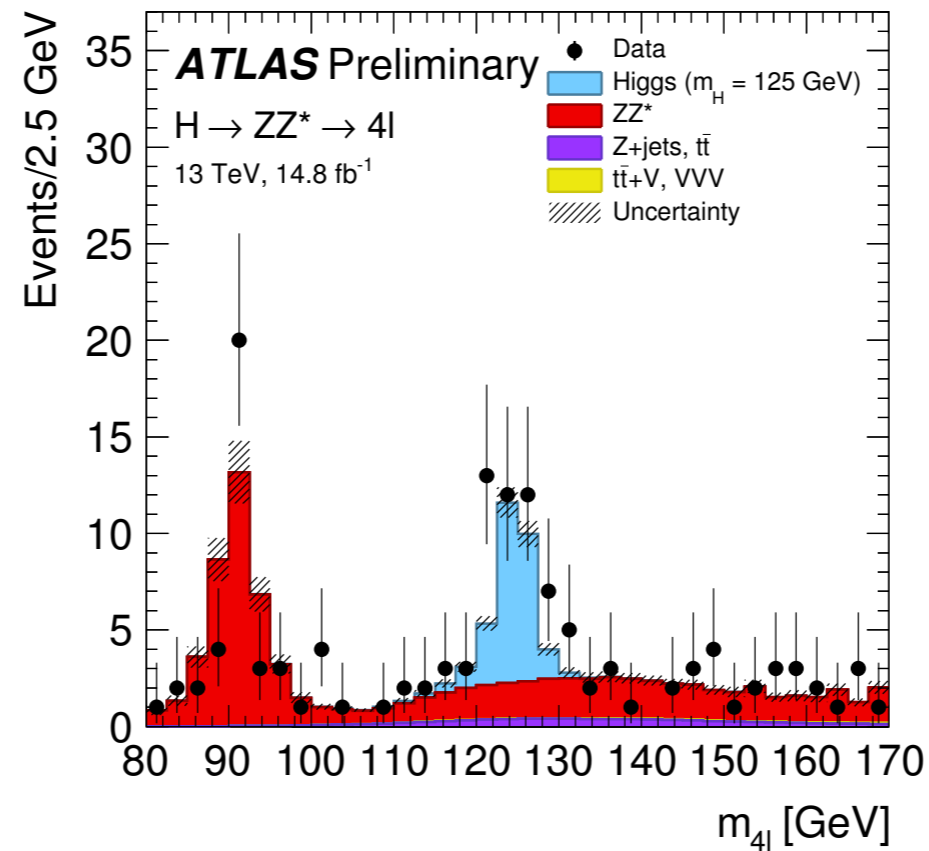


$$H \rightarrow ZZ \rightarrow 4e$$

- The “golden channel”
 - S/B of 2, making it easy to pick out Higgs decays.
- ATLAS provides excellent lepton reconstruction and efficiency
- Exploit properties of the event
 - 4ℓ vertexing constraint in event selection
 - m_{12} (+FSR photons) kinematically constrained to m_Z to improve the resolution.
- Improvements in Run-2
 - IBL provides superior rejection of electron backgrounds
 - Muon p_T cut from 6 to 5 GeV, +8% acceptance



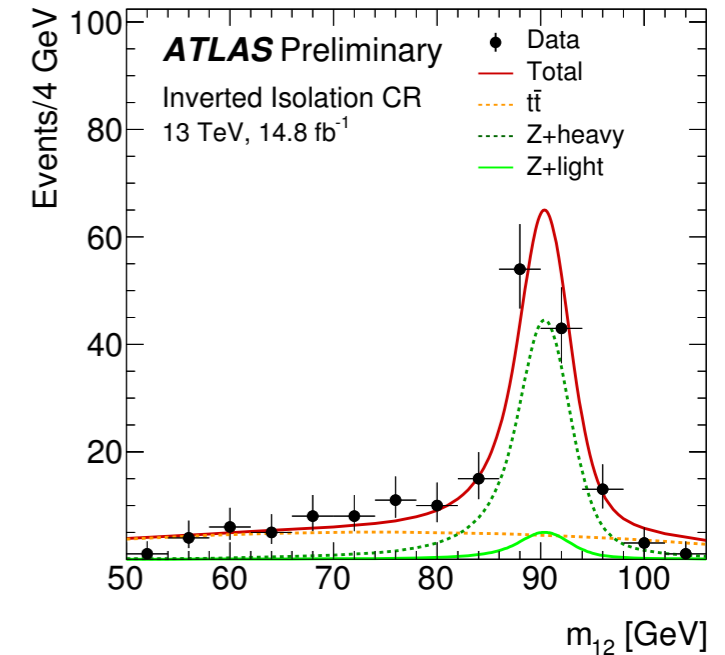
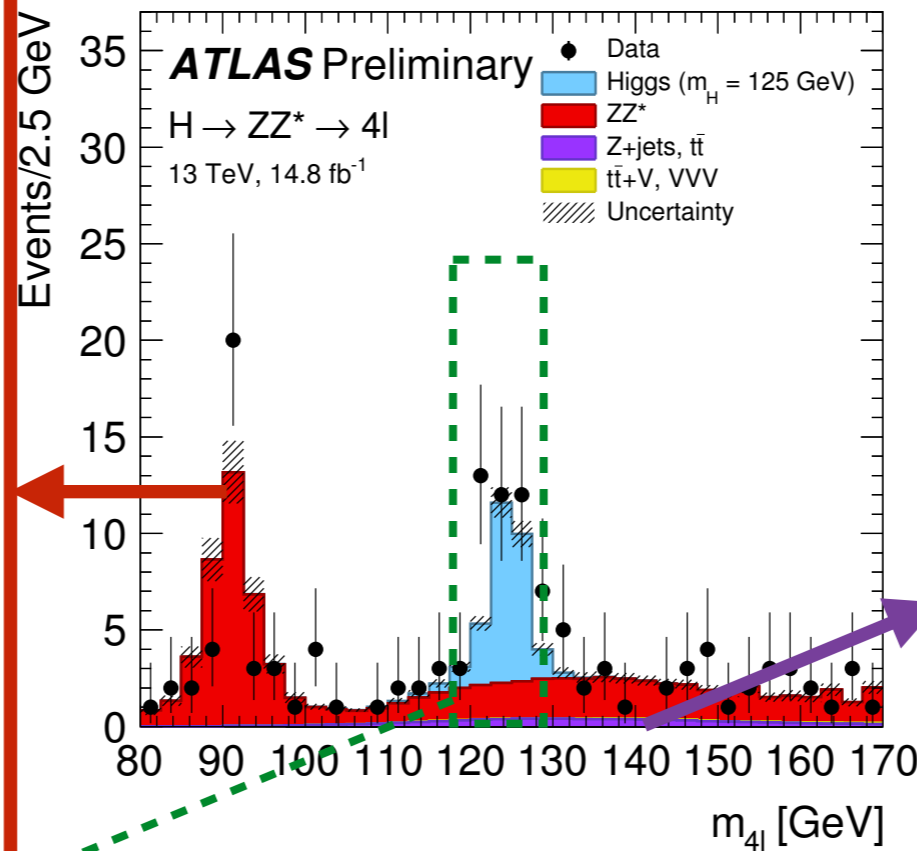
The Higgs Peak



Final State	Signal full mass range	Signal	ZZ^*	$Z + \text{jets}, t\bar{t}$ $t\bar{t}V, VVV, WZ$	S/B	Expected	Observed
4μ	8.8 ± 0.6	8.2 ± 0.6	3.11 ± 0.30	0.31 ± 0.04	2.4	11.6 ± 0.7	16
$2e2\mu$	6.1 ± 0.4	5.5 ± 0.4	2.19 ± 0.21	0.30 ± 0.04	2.2	8.0 ± 0.4	12
$2\mu 2e$	4.8 ± 0.4	4.4 ± 0.4	1.39 ± 0.16	0.47 ± 0.05	2.3	6.2 ± 0.4	10
$4e$	4.8 ± 0.5	4.2 ± 0.4	1.46 ± 0.18	0.46 ± 0.05	2.2	6.1 ± 0.4	6
Total	24.5 ± 1.8	22.3 ± 1.6	8.2 ± 0.8	1.54 ± 0.18	2.3	32.0 ± 1.8	44

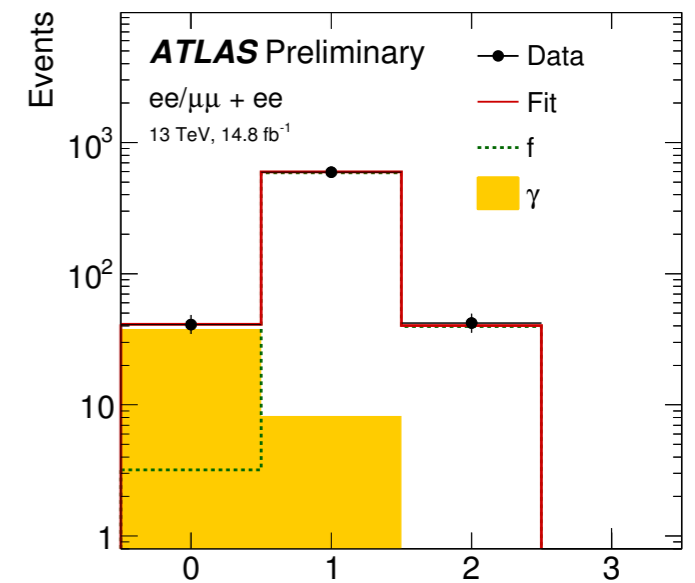
Background Estimates

- Main background is ZZ^* production, taken from simulation.
 - $qq \rightarrow ZZ$ simulated at NLO with POWHEG, QCD and EW corrections as a function of m_{ZZ} .
 - $gg \rightarrow ZZ$ simulated at LO with gg2VV, with a k-factor applied for higher-order QCD effects

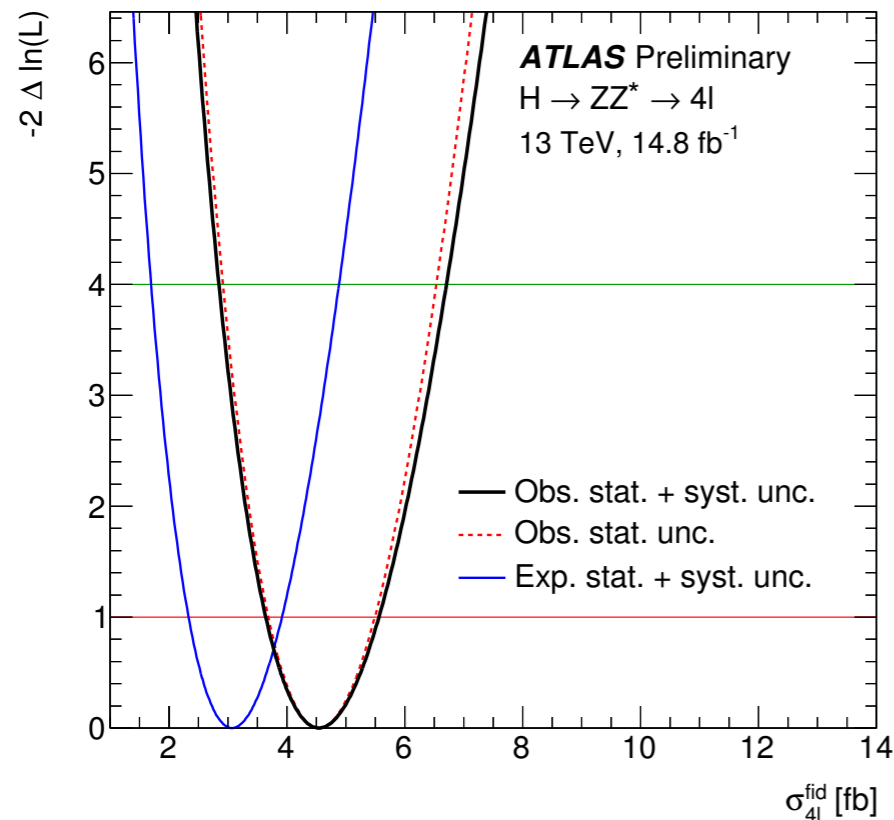


Reducible background from Z+jets and tt estimated using data-driven methods

Final State	Signal	Signal	ZZ^*	Z + jets, $t\bar{t}$ $t\bar{t}V, VVV, WZ$	S/B	Expected	Observed
	full mass range						
4μ	8.8 ± 0.6	8.2 ± 0.6	3.11 ± 0.30	0.31 ± 0.04	2.4	11.6 ± 0.7	16
$2e2\mu$	6.1 ± 0.4	5.5 ± 0.4	2.19 ± 0.21	0.30 ± 0.04	2.2	8.0 ± 0.4	12
$2\mu 2e$	4.8 ± 0.4	4.4 ± 0.4	1.39 ± 0.16	0.47 ± 0.05	2.3	6.2 ± 0.4	10
$4e$	4.8 ± 0.5	4.2 ± 0.4	1.46 ± 0.18	0.46 ± 0.05	2.2	6.1 ± 0.4	6
Total	24.5 ± 1.8	22.3 ± 1.6	8.2 ± 0.8	1.54 ± 0.18	2.3	32.0 ± 1.8	44



Fiducial Cross-Section



Final state	measured σ_{fid} [fb]	$\sigma_{\text{fid,SM}}$ [fb]
4μ	$1.28^{+0.48}_{-0.40}$	$0.93^{+0.06}_{-0.08}$
$4e$	$0.81^{+0.51}_{-0.38}$	$0.73^{+0.05}_{-0.06}$
$2\mu 2e$	$1.29^{+0.58}_{-0.46}$	$0.67^{+0.04}_{-0.04}$
$2e 2\mu$	$1.10^{+0.49}_{-0.40}$	$0.76^{+0.05}_{-0.06}$

$$\sigma_{\text{tot}} = 81^{+18}_{-16} \text{ pb}$$

$$\sigma_{\text{tot,SM}} = 55.5^{+3.8}_{-4.4} \text{ pb}$$

Uncertainties are still statistically dominated.

Compatible with SM at 1.6σ .

- Fiducial cross-section is independent of assumptions about acceptance factors or branching ratios

- Reduces model dependence

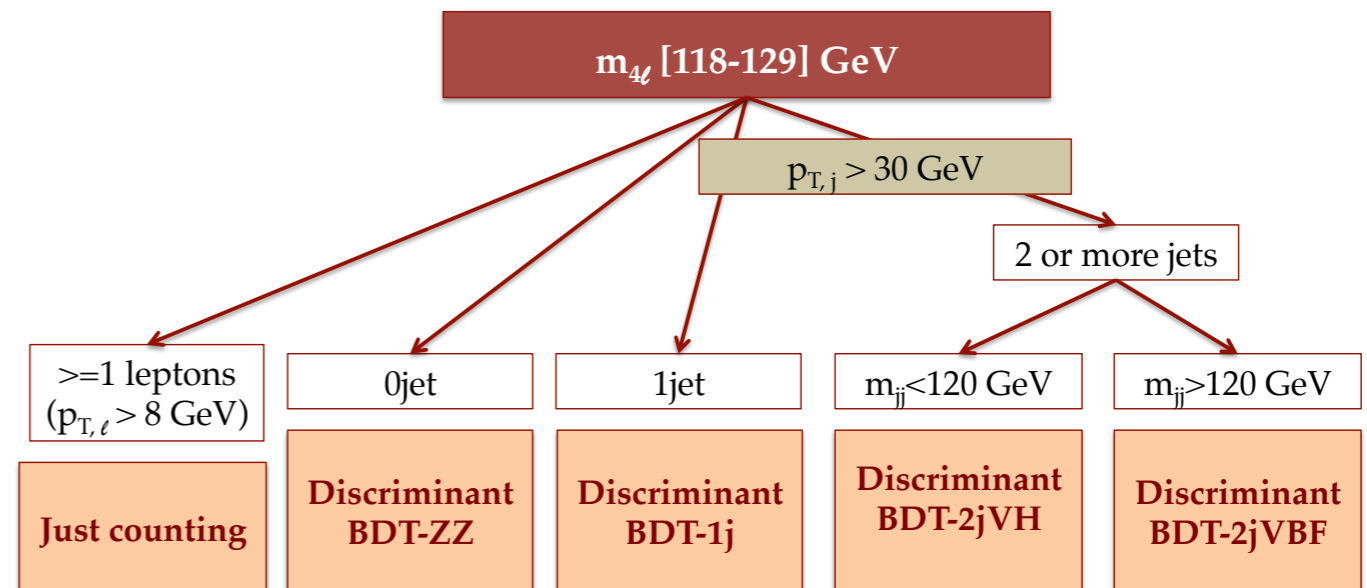
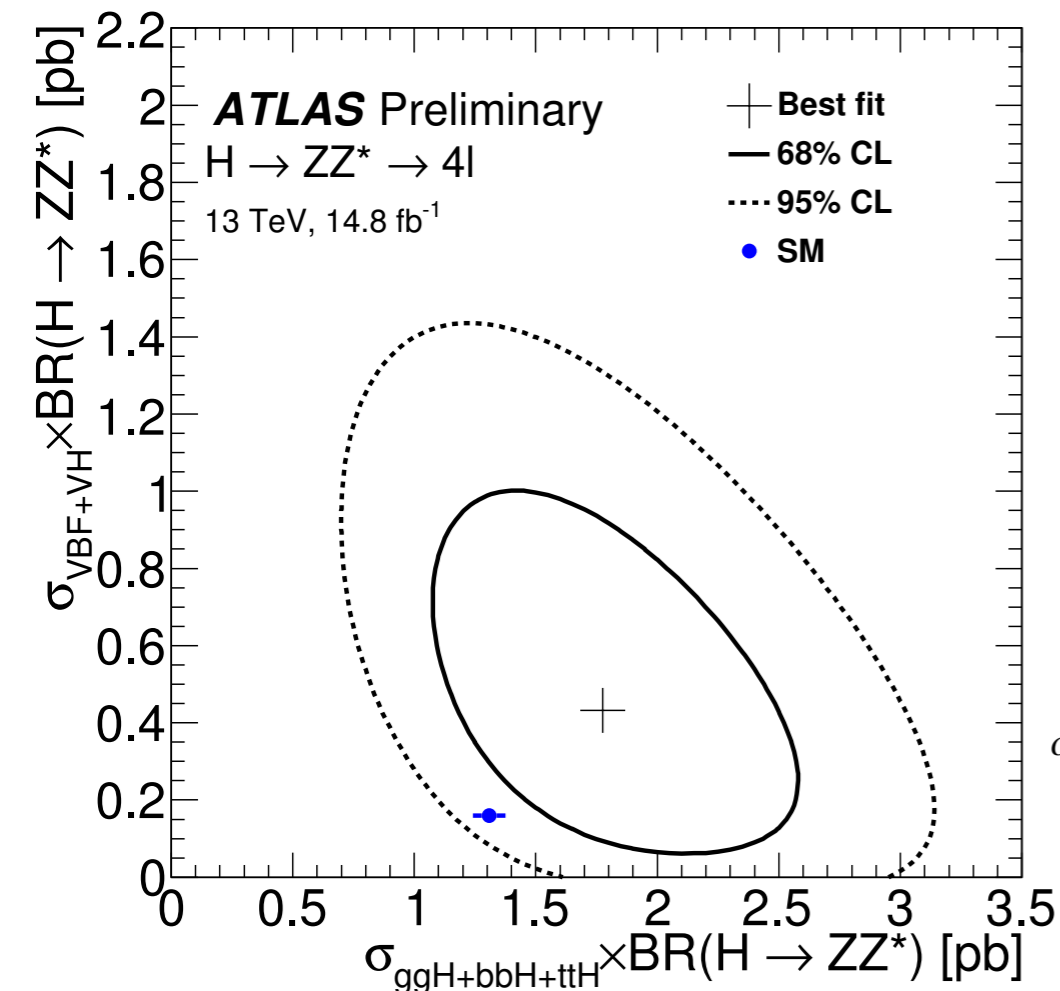
- Only need to correct for detector efficiencies and resolution

- Fiducial cross-section is obtained from a likelihood fit to the $m_{4\ell}$ distribution for $115 < m_{4\ell} < 130$ GeV.

- Total cross-section is then obtained assuming SM BR and acceptance.

$$\sigma_{\text{channel}}^{\text{fid}} = \frac{N_s}{\mathcal{C} \cdot \mathcal{L}_{\text{int}}}$$

Cross-sections by Production Mode



$$\sigma_{\text{ggF}+\text{bb}\bar{\text{b}}\text{H}+\text{tt}\bar{\text{t}}\text{H}} \cdot \mathcal{B}(H \rightarrow ZZ^*) = 1.80^{+0.49}_{-0.44} \text{ pb}$$

$$\sigma_{\text{VBF}} \cdot \mathcal{B}(H \rightarrow ZZ^*) = 0.37^{+0.28}_{-0.21} \text{ pb}$$

$$\sigma_{\text{VH}} \cdot \mathcal{B}(H \rightarrow ZZ^*) = 0^{+0.15} \text{ pb}$$

$$\sigma_{\text{SM},\text{ggF}+\text{bb}\bar{\text{b}}\text{H}+\text{tt}\bar{\text{t}}\text{H}} \cdot \mathcal{B}(H \rightarrow ZZ^*) = 1.31 \pm 0.07 \text{ pb}$$

$$\sigma_{\text{SM},\text{VBF}} \cdot \mathcal{B}(H \rightarrow ZZ^*) = 0.100 \pm 0.003 \text{ pb}$$

$$\sigma_{\text{SM},\text{VH}} \cdot \mathcal{B}(H \rightarrow ZZ^*) = 0.059 \pm 0.002 \text{ pb}$$

Compatibility to the SM prediction
 $\sigma_{\text{ggF}+\text{bb}\bar{\text{b}}\text{H}+\text{tt}\bar{\text{t}}\text{H}} \cdot \mathcal{B}(H \rightarrow ZZ^*)$ is 1.1σ and $\sigma_{\text{VBF}} \cdot \mathcal{B}(H \rightarrow ZZ^*)$ is 1.4σ .

- Events in the $118 < m_{4\ell} < 129$ GeV range are sorted into exclusive categories.
 - Except in VH-leptonic, a BDT is used to enhance sensitivity.
- Signal obtained from a likelihood fit to the BDT output.
 - The cross-section is then obtained assuming $m_H = 125.09$ GeV.

BSM Sensitivity

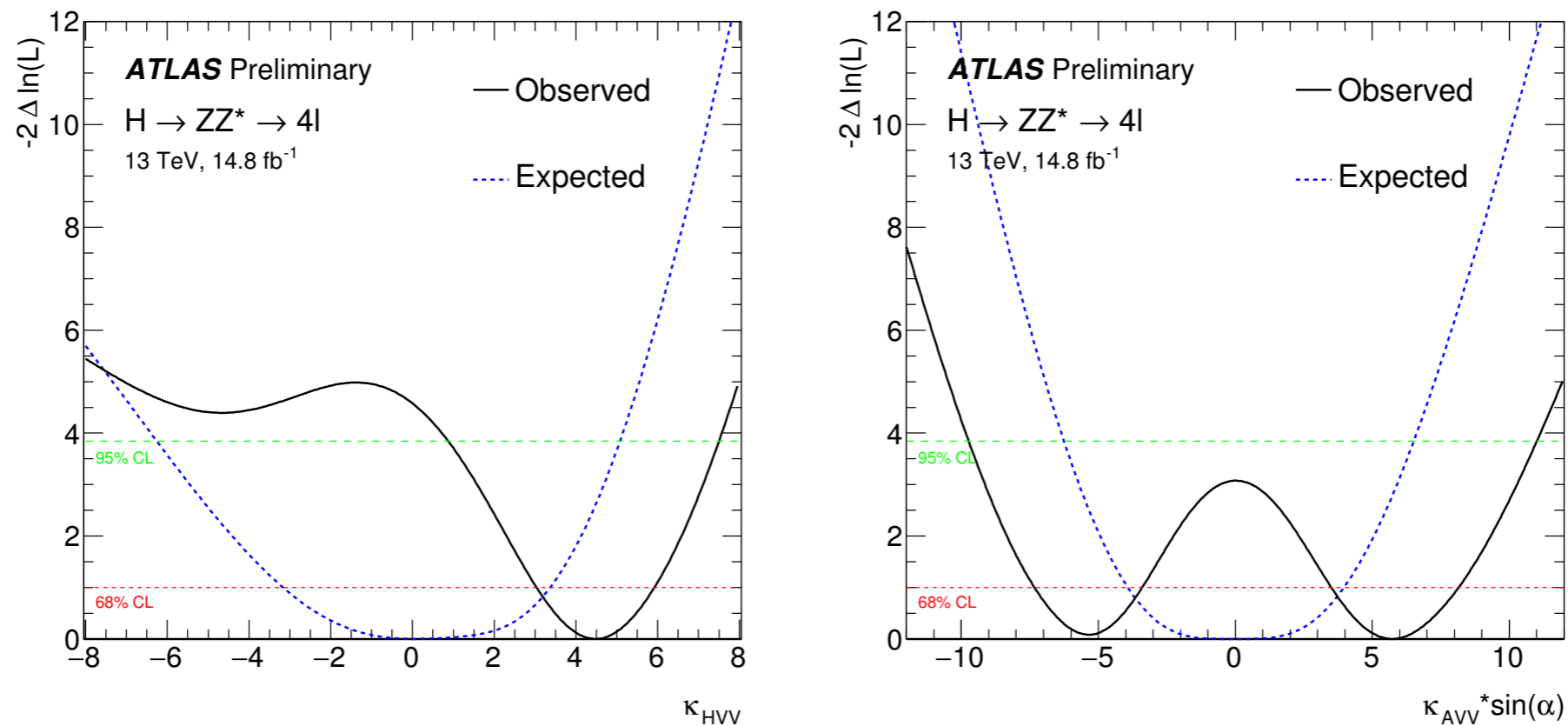
$$\mathcal{L}_0^V = \left\{ c_\alpha \kappa_{\text{SM}} \left[\frac{1}{2} g_{HZZ} Z_\mu Z^\mu + g_{HWW} W_\mu^+ W^{-\mu} \right] \right. \\
- \frac{1}{4} [c_\alpha \kappa_{H\gamma\gamma} g_{H\gamma\gamma} A_{\mu\nu} A^{\mu\nu} + s_\alpha \kappa_{A\gamma\gamma} g_{A\gamma\gamma} A_{\mu\nu} \tilde{A}^{\mu\nu}] \\
- \frac{1}{2} [c_\alpha \kappa_{HZ\gamma} g_{HZ\gamma} Z_{\mu\nu} A^{\mu\nu} + s_\alpha \kappa_{AZ\gamma} g_{AZ\gamma} Z_{\mu\nu} \tilde{A}^{\mu\nu}] \\
- \frac{1}{4} [c_\alpha \kappa_{Hgg} g_{Hgg} G_{\mu\nu}^a G^{a,\mu\nu} + s_\alpha \kappa_{Agg} g_{Agg} G_{\mu\nu}^a \tilde{G}^{a,\mu\nu}] \\
- \frac{1}{4} \frac{1}{\Lambda} [c_\alpha \kappa_{HZZ} Z_{\mu\nu} Z^{\mu\nu} + s_\alpha \kappa_{AZZ} Z_{\mu\nu} \tilde{Z}^{\mu\nu}] \\
- \frac{1}{2} \frac{1}{\Lambda} [c_\alpha \kappa_{HWW} W_{\mu\nu}^+ W^{-\mu\nu} + s_\alpha \kappa_{AWW} W_{\mu\nu}^+ \tilde{W}^{-\mu\nu}] \\
\left. - \frac{1}{\Lambda} c_\alpha [\kappa_{H\partial\gamma} Z_\nu \partial_\mu A^{\mu\nu} + \kappa_{H\partial Z} Z_\nu \partial_\mu Z^{\mu\nu} + (\kappa_{H\partial W} W_\nu^+ \partial_\mu W^{-\mu\nu} + h.c.)] \right\} X_0$$

JHEP 11 (2013) 043

- Madgraph5_aMC@NLO is used to generate template samples.
- Then the morphing technique is used to obtain predictions for any value of the BSM couplings.

- Exclusive event category yields are also used to probe for BSM interactions.
- BSM effects are parameterized using the Higgs characterization model
 - BSM couplings k_{HVV} (scalar) and k_{AVV} (pseudo-scalar) are studied (assuming $\cos(\alpha)=1$ and the couplings are the same for W and Z).
 - VBF and VH production yields scale with k_{BSM}^4 .

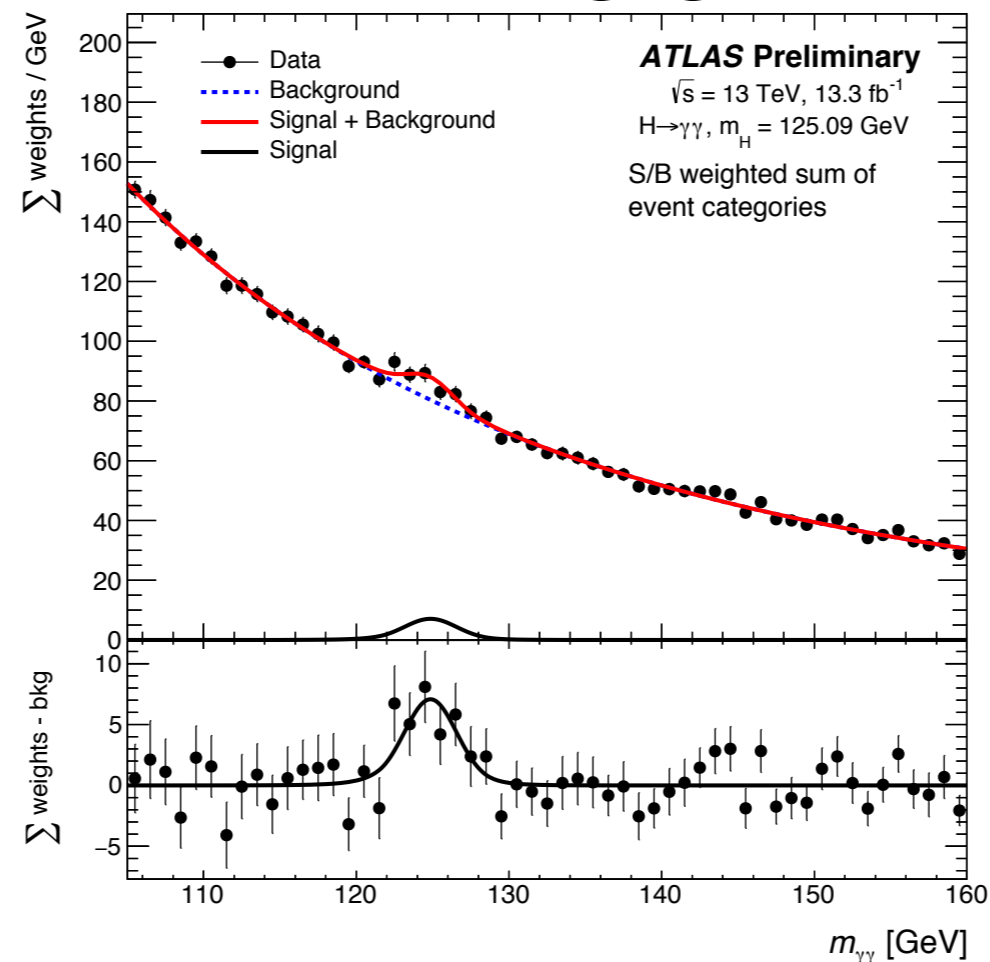
BSM Sensitivity



Not excluded range at 95% CL	κ_{HVV}		$\kappa_{AVV} \cdot \sin \alpha$	
	expected	observed	expected	observed
	[-6.3, 5.1]	[0.9, 7.5]	[-6.3, 6.5]	[-9.7, 11.0]

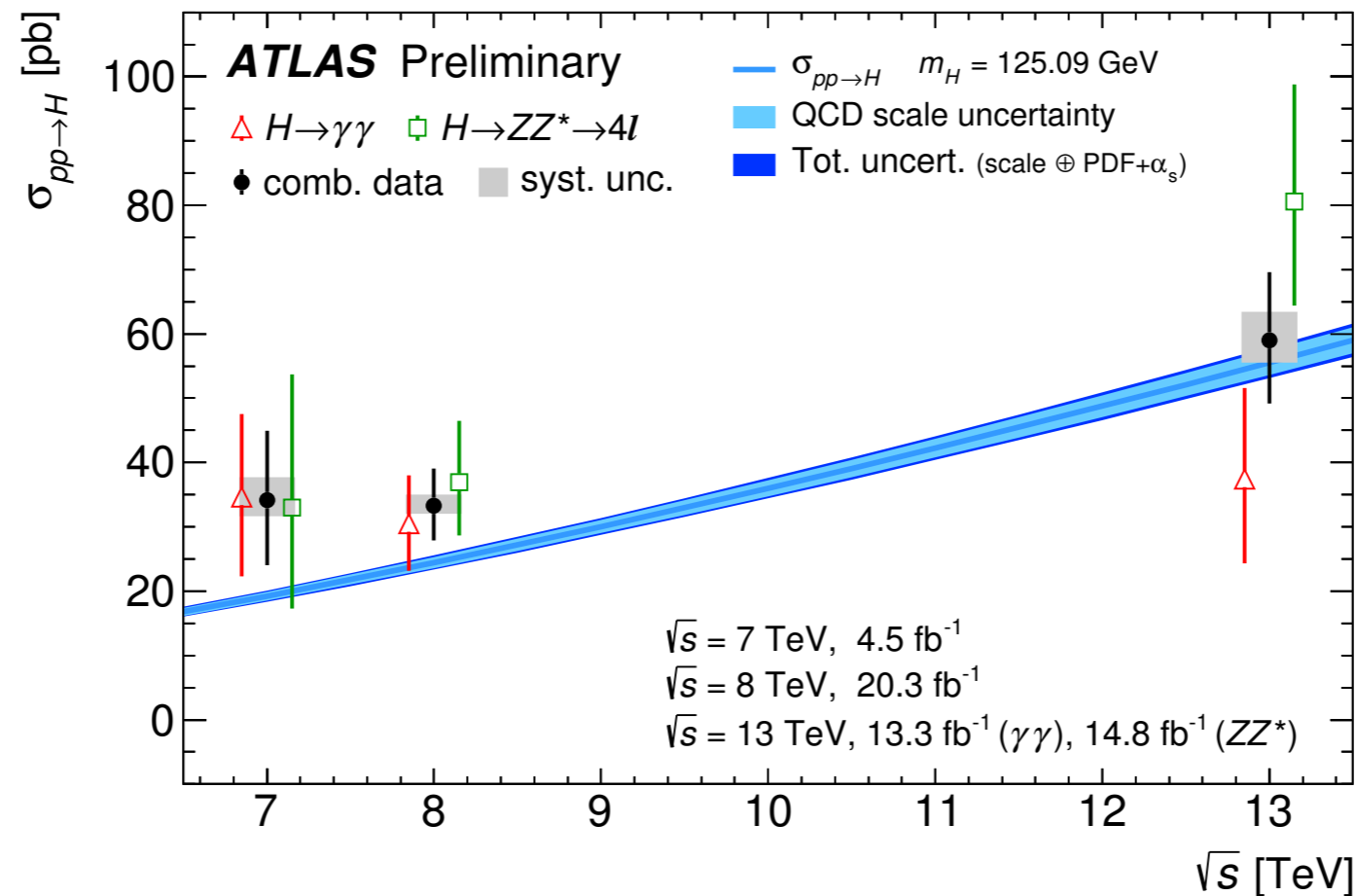
- Limits are derived from a fit to the yields (no kinematic information is used), considering one coupling at a time.
 - ggF production is fixed to the SM value for the fit.
- Limits are weaker than SM expectation.
 - κ_{HVV} is 2.1σ compatible with 0 and κ_{AVV} 1.8σ .

$$H \rightarrow \gamma\gamma$$



- Events are split into 13 different exclusive categories, based on
 - Production modes
 - Decay products of particles produced with the Higgs
- The fiducial measurement uses the inclusive distribution instead.
- Background shape is parametrized in each category from MC, and fit to data.
- Signal is extracted from a simultaneous fit to the $m_{\gamma\gamma}$ distribution across all categories.

Signal Strength and Total Cross-Section

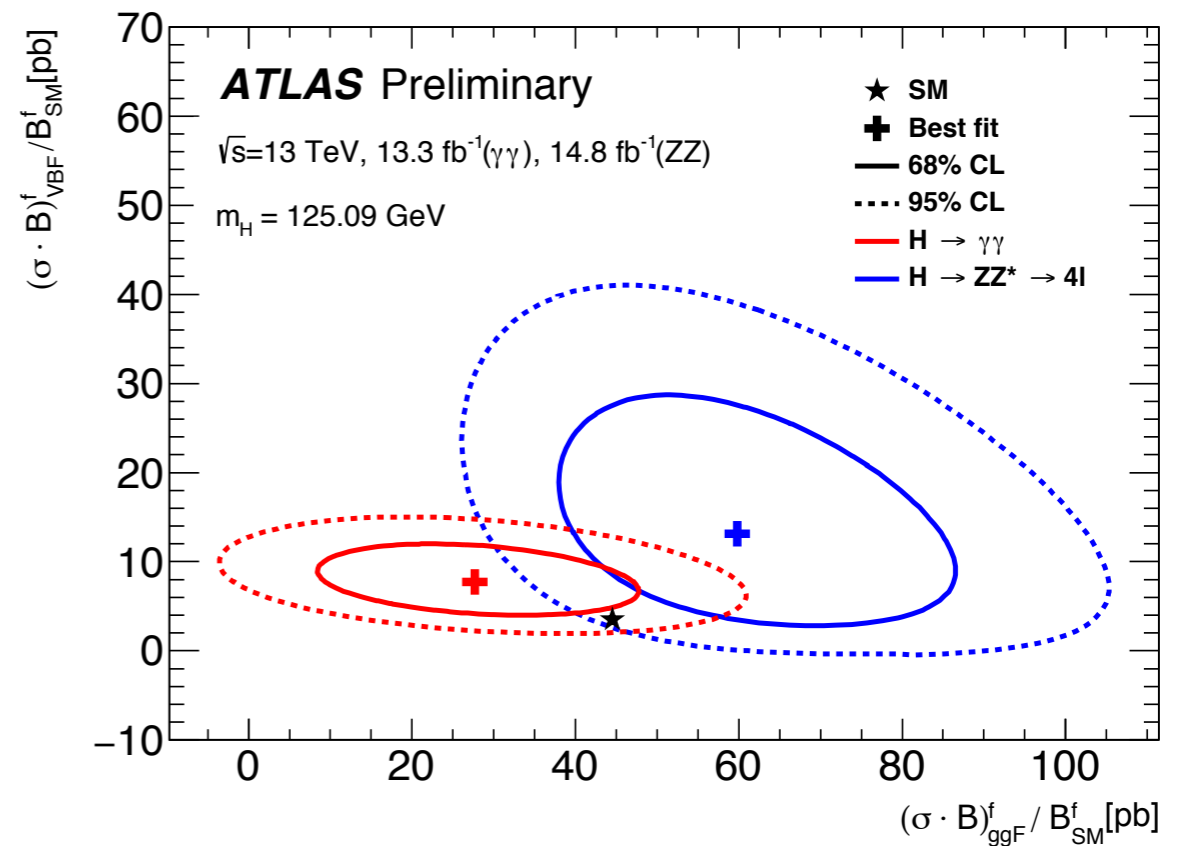
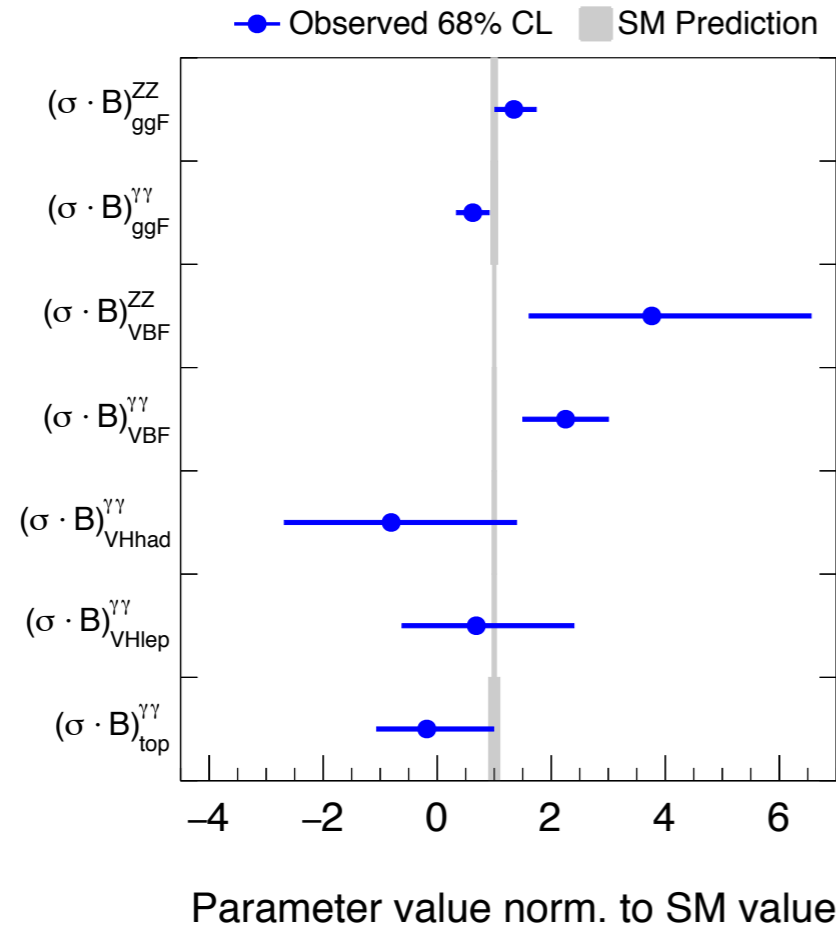


$$\mu = 1.13^{+0.18}_{-0.17}$$

No deviations from the SM prediction are observed in the total cross-section or global signal strength.

Combined $\gamma\gamma$ - 4ℓ Results

ATLAS Preliminary $m_H=125.09$ GeV
 $\sqrt{s}=13$ TeV, 13.3 fb^{-1} ($\gamma\gamma$), 14.8 fb^{-1} (ZZ)

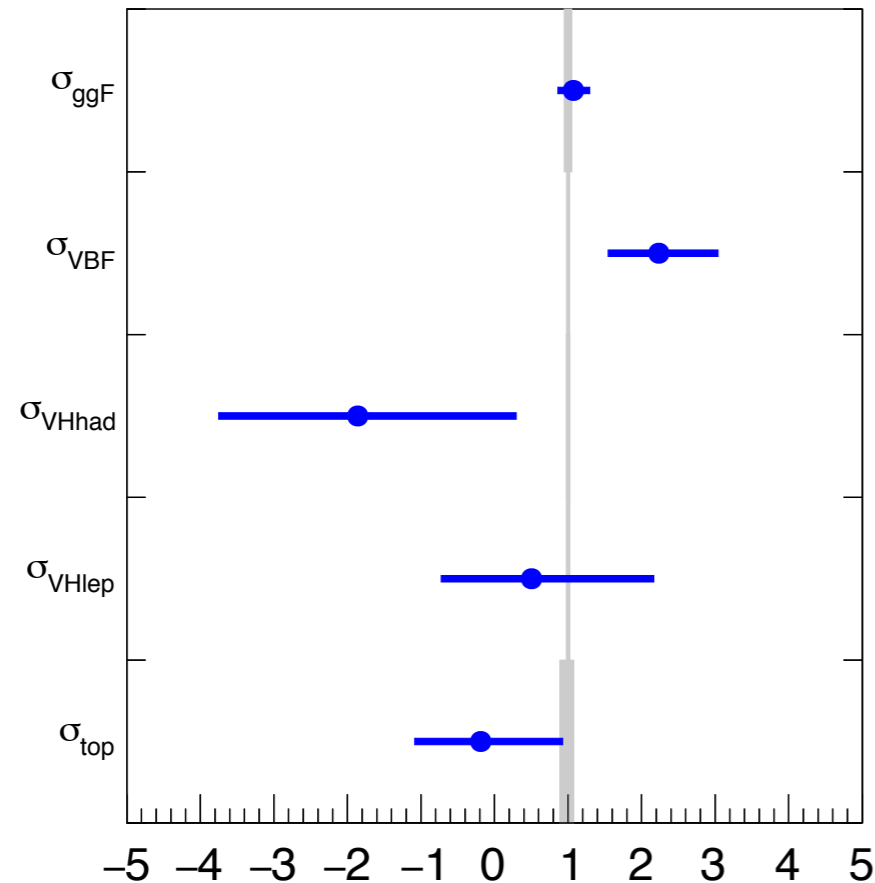


- Each $\sigma_i \times \text{BR}^f$ parameter is treated as independent in the fit: results are shown upper left.
- Upper right plot shows the fit result divided by the SM BR.

Combined Cross-section Results

ATLAS Preliminary $m_H=125.09$ GeV
 $\sqrt{s}=13$ TeV, 13.3 fb^{-1} ($\gamma\gamma$), 14.8 fb^{-1} (ZZ)

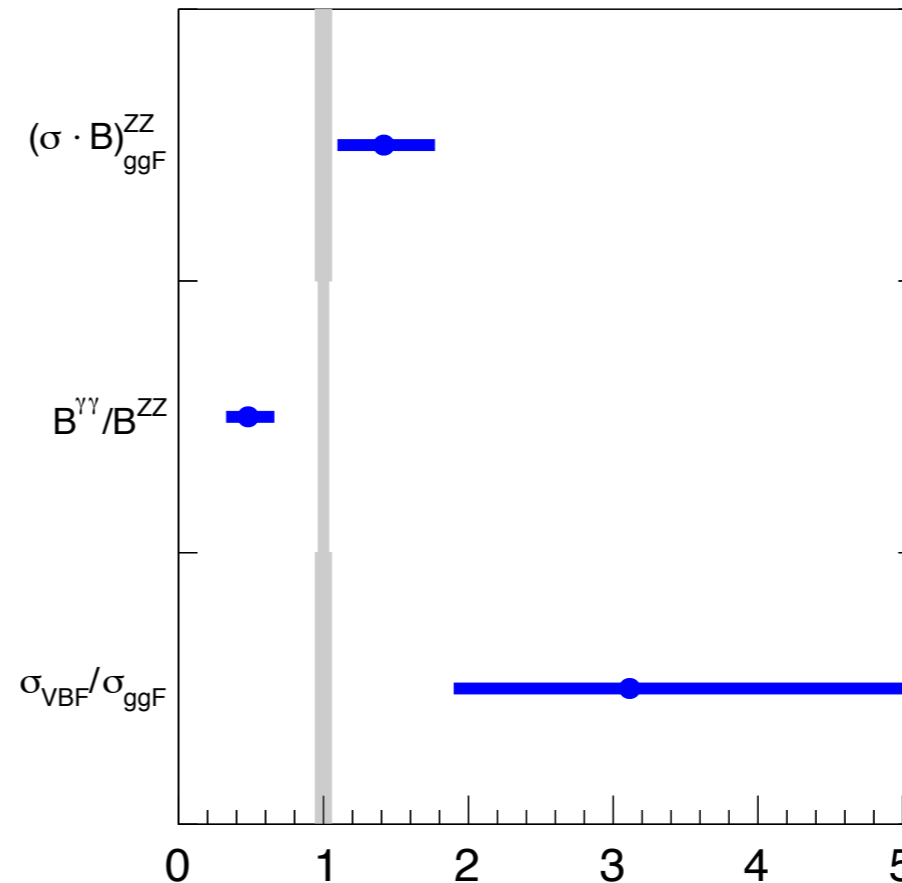
—●— Observed 68% CL ■ SM Prediction



Parameter value norm. to SM value

ATLAS Preliminary $m_H=125.09$ GeV
 $\sqrt{s}=13$ TeV, 13.3 fb^{-1} ($\gamma\gamma$), 14.8 fb^{-1} (ZZ)

—●— Observed 68% CL ■ SM Prediction



Parameter value norm. to SM value

- Left: BRs are assumed to take their SM values.
- Right: the $\sigma_i \times BR^f$ values are parameterized in terms of the ratios σ_i/σ_{ggF} and BR^f/BR^{ZZ} .
- All results are consistent with SM expectations.

Summary and Conclusions

- The Higgs is rediscovered at $\sqrt{s}=13$ TeV!
- Utilizing the 4ℓ decay channel, a number of measurements of Higgs properties are made with the new 13 TeV dataset.
 - Additionally, possible sources of BSM behavior are probed.
 - No significant deviations from the SM are observed.
- Further precision can be obtained by combining measurements in the 4ℓ channel with those in the $\gamma\gamma$ channel.
 - Again, no significant deviations from the SM are found.
- Since ICHEP 2016, our 13 TeV dataset has more than doubled.
 - New, more precise tests of the SM are on the way.

Backup

4 ℓ Event Selection

PHYSICS OBJECTS

ELECTRONS

Loose Likelihood quality electrons with hit in innermost layer, $E_T > 7$ GeV and $|\eta| < 2.47$

MUONS

Loose identification

Calo-tagged muons with $p_T > 15$ GeV and $|\eta| < 0.1$

Combined, stand-alone (with ID hits if available) and segment tagged muons with $p_T > 5$ GeV

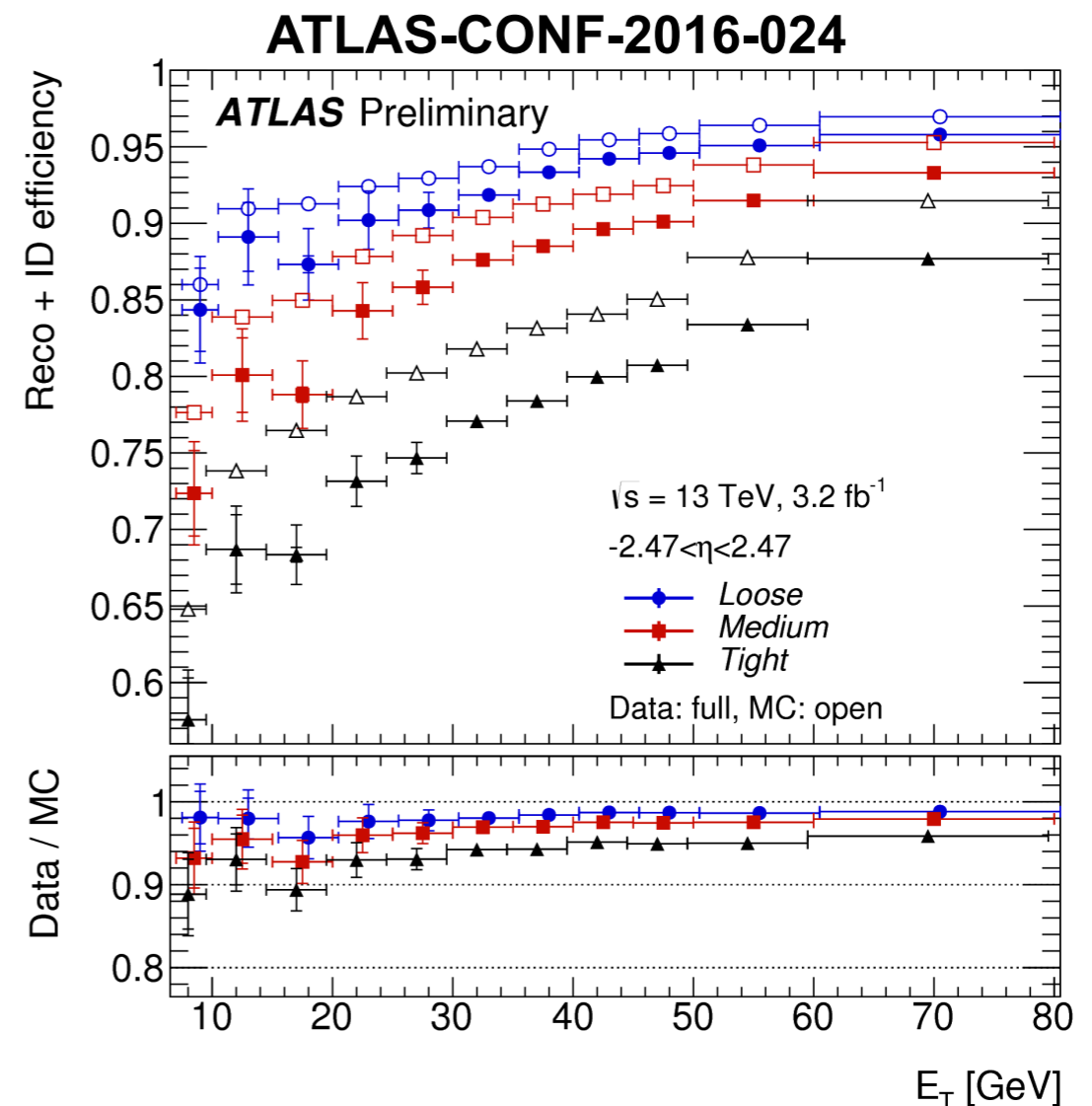
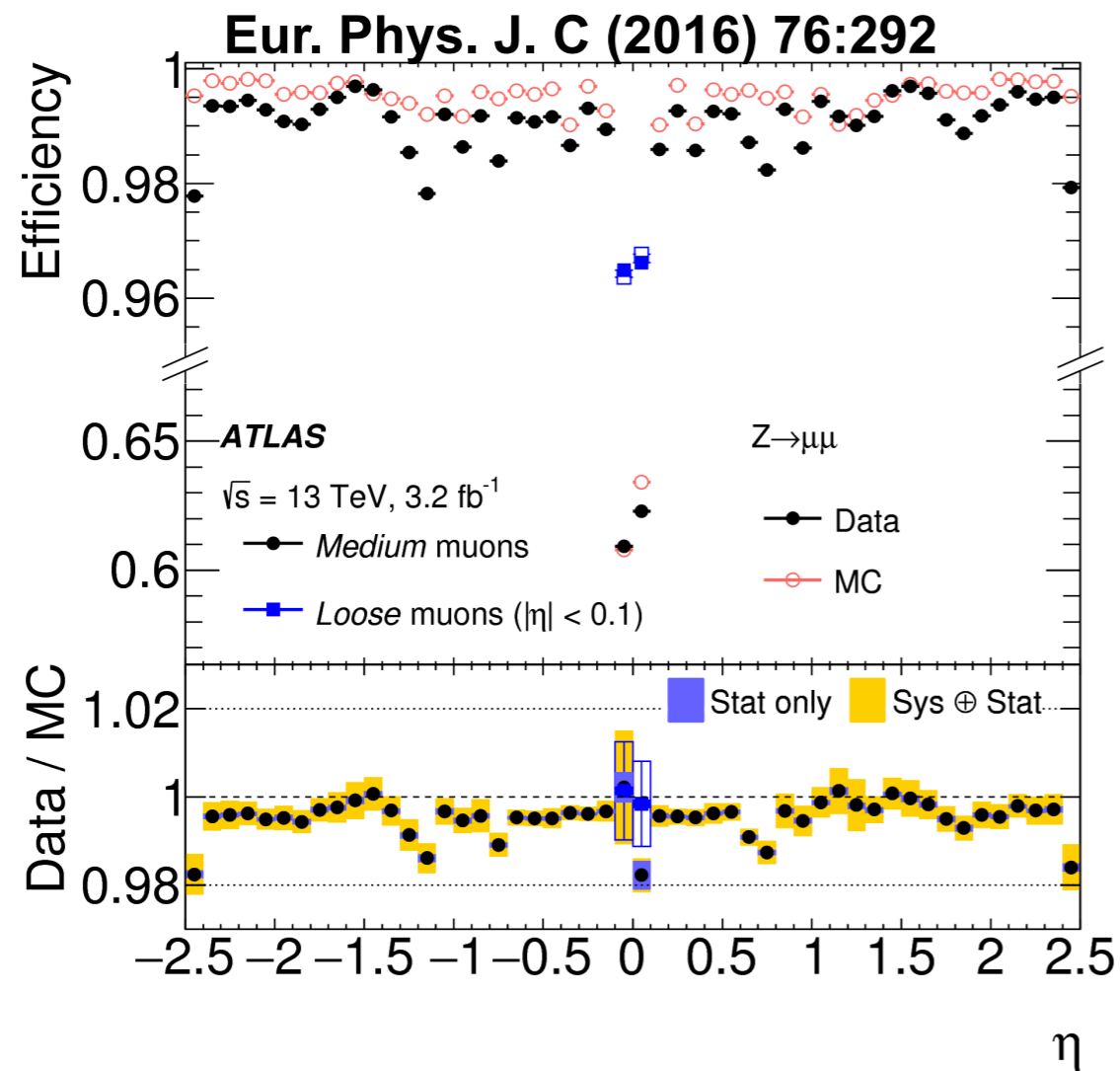
JETS

anti- k_T jets with $p_T > 30$ GeV, $|\eta| < 4.5$ and passing pile-up jet rejection requirements

EVENT SELECTION

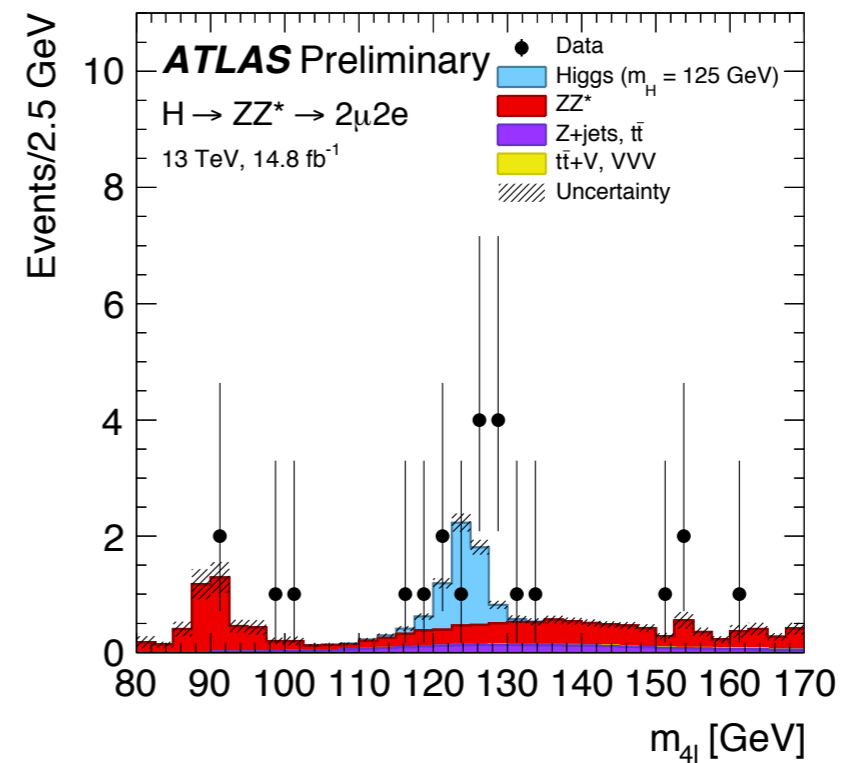
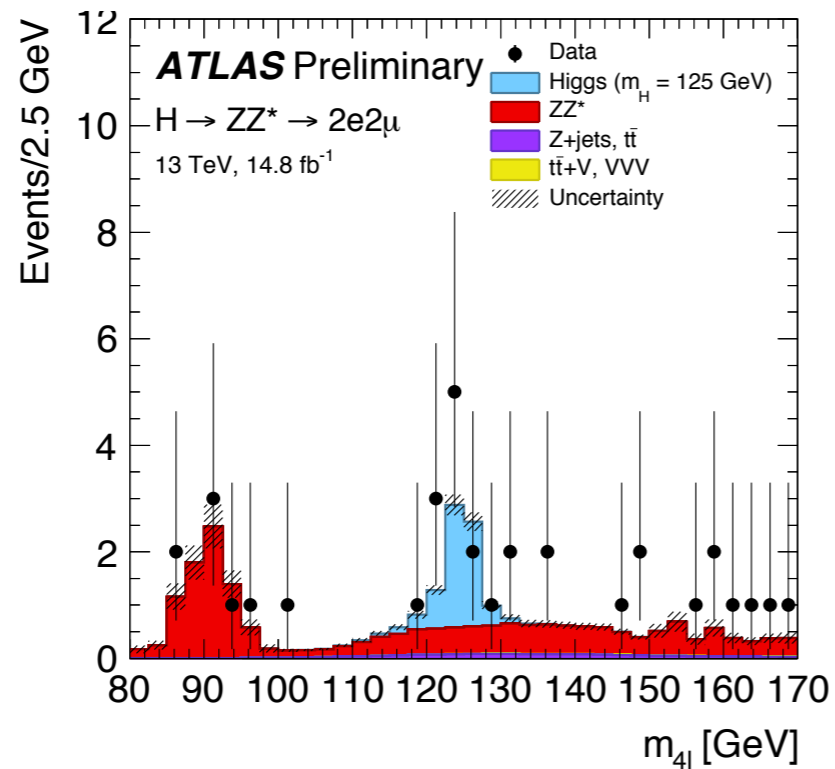
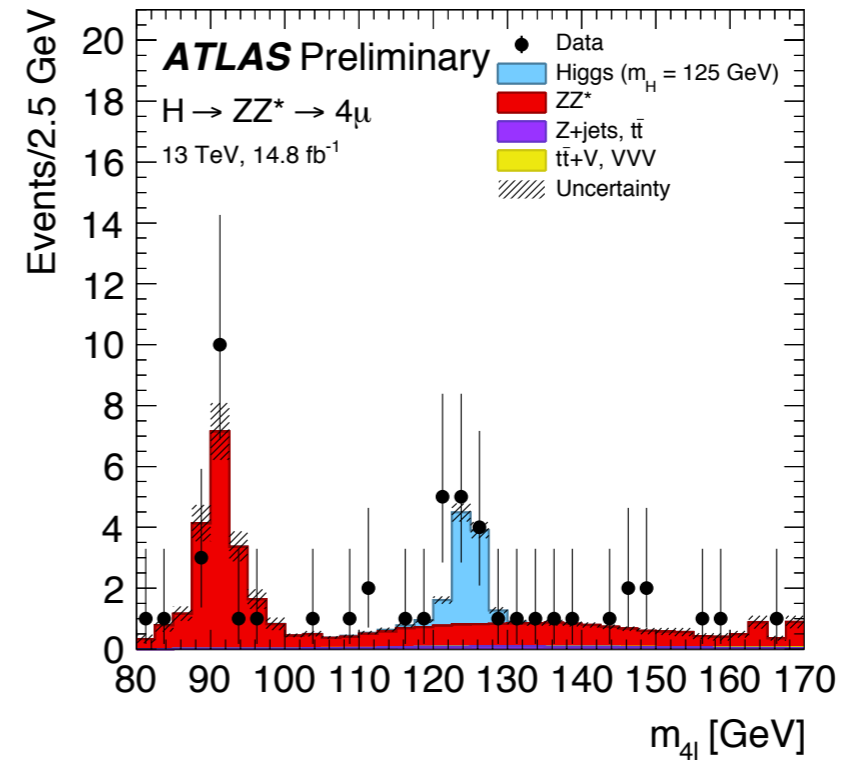
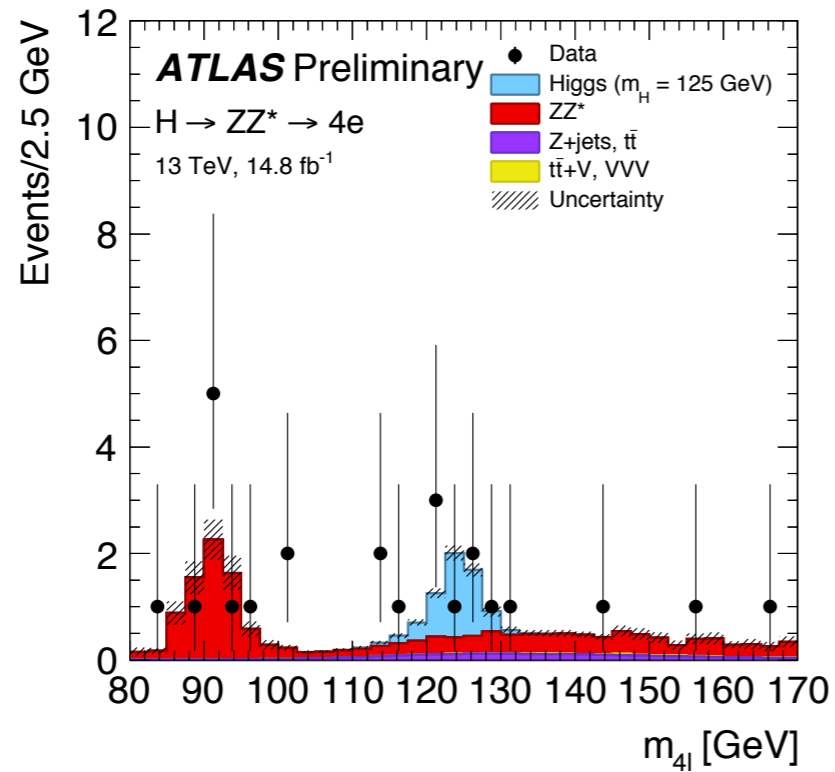
QUADRUPLET SELECTION	<p>Require at least one quadruplet of leptons consisting of two pairs of same-flavour opposite-charge leptons fulfilling the following requirements:</p> <p>p_T thresholds for three leading leptons in the quadruplet - 20, 15 and 10 GeV</p> <p>Maximum one calo-tagged or standalone muon per quadruplet</p> <p>Select best quadruplet to be the one with the (sub)leading dilepton mass (second) closest the Z mass</p> <p>Leading di-lepton mass requirement: $50 \text{ GeV} < m_{12} < 106 \text{ GeV}$</p> <p>Sub-leading di-lepton mass requirement: $12 < m_{34} < 115 \text{ GeV}$</p> <p>Remove quadruplet if alternative same-flavour opposite-charge di-lepton gives $m_{\ell\ell} < 5 \text{ GeV}$</p> <p>$\Delta R(\ell, \ell') > 0.10$ (0.20) for all same (different) flavour leptons in the quadruplet</p>
ISOLATION	<p>Contribution from the other leptons of the quadruplet is subtracted</p> <p>Muon track isolation ($\Delta R \leq 0.30$): $\Sigma p_T / p_T < 0.15$</p> <p>Muon calorimeter isolation ($\Delta R \leq 0.20$): $\Sigma E_T / p_T < 0.30$</p> <p>Electron track isolation ($\Delta R \leq 0.20$): $\Sigma E_T / E_T < 0.15$</p> <p>Electron calorimeter isolation ($\Delta R \leq 0.20$): $\Sigma E_T / E_T < 0.20$</p>
IMPACT PARAMETER SIGNIFICANCE	<p>Apply impact parameter significance cut to all leptons of the quadruplet.</p> <p>For electrons : $d_0 / \sigma_{d_0} < 5$</p> <p>For muons : $d_0 / \sigma_{d_0} < 3$</p>
VERTEX SELECTION	<p>Require a common vertex for the leptons</p> <p>$\chi^2 / \text{ndof} < 6$ for 4μ and < 9 for others.</p>

Electron and Muon Performance

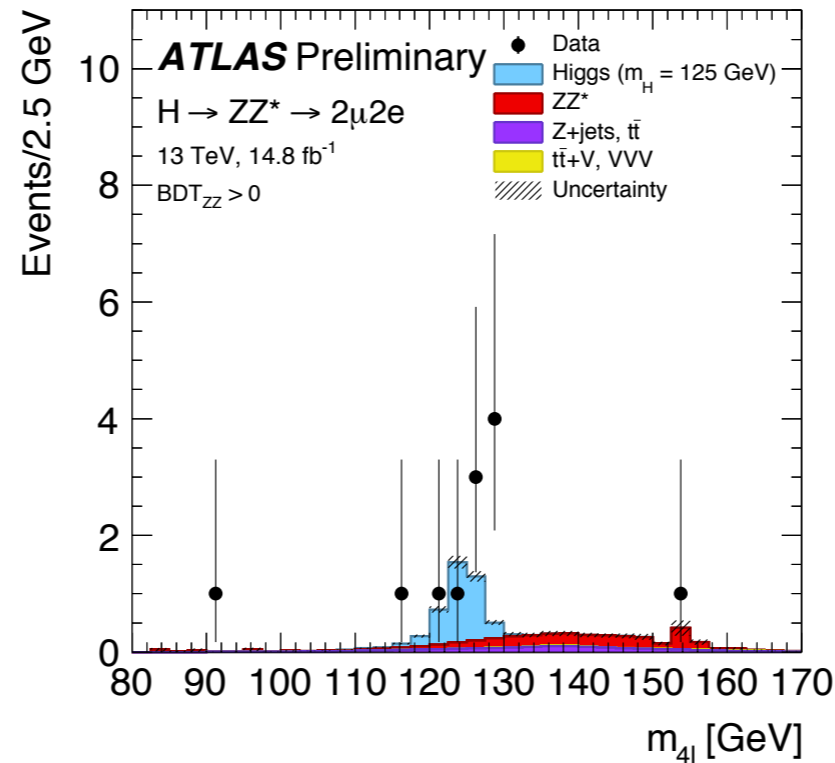
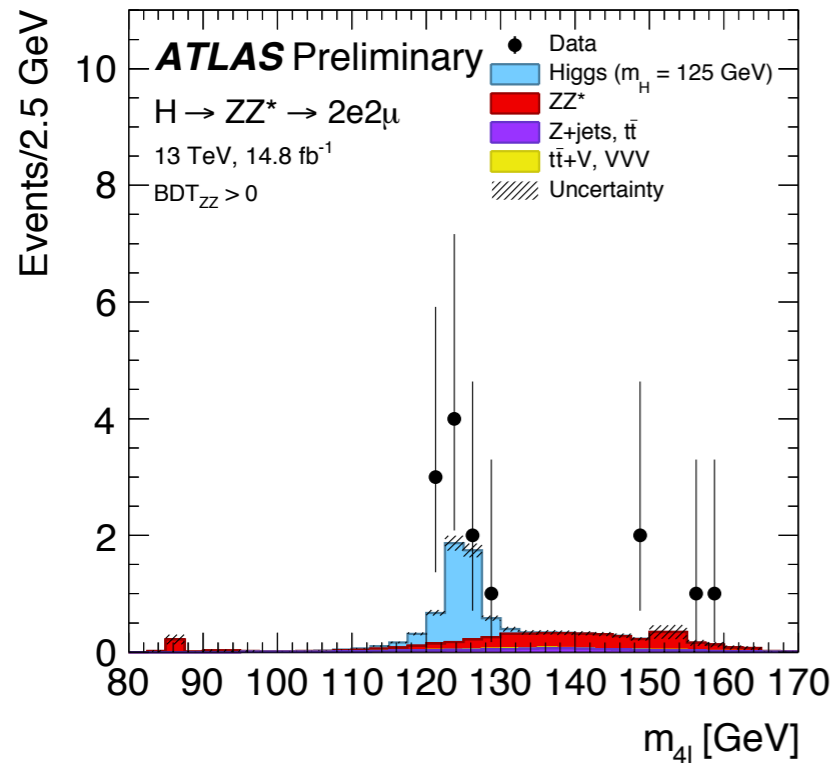
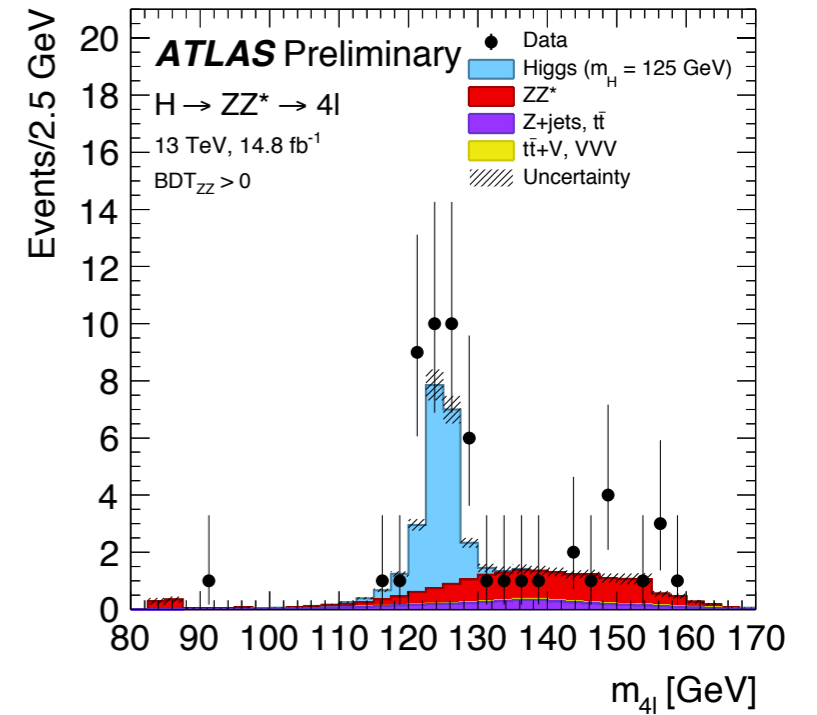
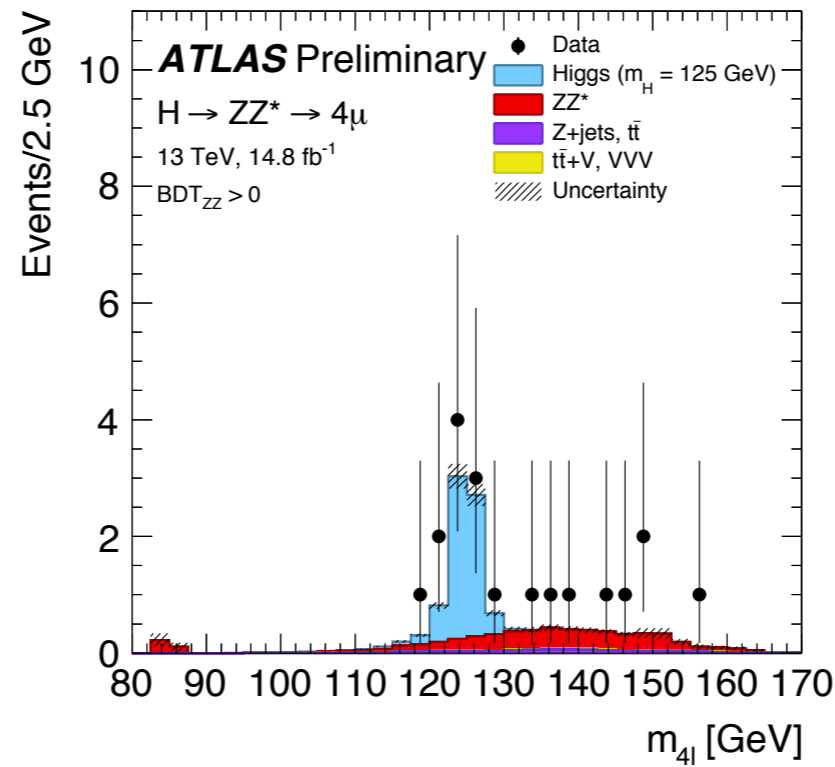
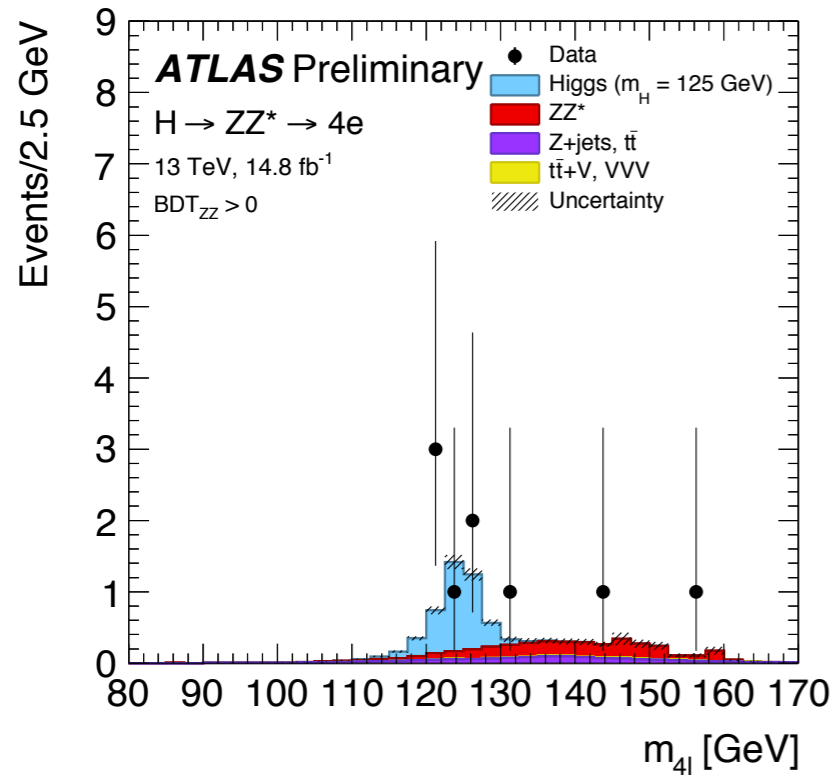


Detector performance well understood, data used to correct simulation.

$m_{4\ell}$ distributions per channel



$m_{4\ell}$ distributions per channel ($\text{BDT}_{ZZ} > 0$)



Fiducial Volume

Lepton definition	
Muons: $p_T > 5 \text{ GeV}, \eta < 2.7$	Electrons: $p_T > 7 \text{ GeV}, \eta < 2.47$
Pairing	
Leading pair:	SFOS lepton pair with smallest $ m_Z - m_{\ell\ell} $
Sub-leading pair:	Remaining SFOS lepton pair with smallest $ m_Z - m_{\ell\ell} $
Event selection	
Lepton kinematics:	Leading lepton $p_T > 20, 15, 10 \text{ GeV}$
Mass requirements:	$50 < m_{12} < 106 \text{ GeV}; 12 < m_{34} < 115 \text{ GeV}$
Lepton separation:	$\Delta R(\ell_i, \ell_j) > 0.1(0.2)$ for same (opposite) flavor leptons
J/ψ veto:	$m(\ell_i, \ell_j) > 5 \text{ GeV}$ for all SFOS lepton pairs
Mass window:	$115 < m_{4\ell} < 130 \text{ GeV}$

$$N_{Data}(m_{4\ell})_i = \mathcal{L}_{int} \cdot \sigma^{\text{tot}} \cdot \mathcal{B}(H \rightarrow 4\ell).$$

$$\left(f_i \cdot PDF(m_{4\ell})_{sig,i} \cdot \sum_{proc} (r_{proc} \cdot \mathcal{A}_{proc,i} \cdot C_{proc,i}) + PDF(m_{4\ell})_{bkg,i} \cdot N_{bkg,i} \right).$$

Acceptance factors \mathcal{A} [%]					
Decay Channel	Production mode				
	ggF	VBF	WH	ZH	$t\bar{t}H$
4μ	50.9	55.0	43.8	46.5	53.6
$4e$	39.6	43.9	34.4	36.0	44.6
$2\mu 2e$	40.0	42.9	34.0	35.5	42.4
$2e 2\mu$	45.9	48.6	38.0	40.4	47.2

Correction factors C [%]					
Decay Channel	Production mode				
	ggF	VBF	WH	ZH	$t\bar{t}H$
4μ	62.6	64.2	60.8	60.5	41.8
$4e$	42.1	43.2	43.0	42.7	38.7
$2\mu 2e$	46.9	50.9	49.1	48.6	41.7
$2e 2\mu$	53.1	54.7	51.8	50.2	36.7

Exclusive Categories Yields

Table 12: The expected and observed yields in the 0-jet, 1-jet, 2-jet with $m_{jj} > 120$ GeV (*VBF-enriched*), 2-jet with $m_{jj} < 120$ GeV (*VH-enriched*) and VH-leptonic categories. The yields are given for the different production modes, assuming $m_H = 125$ GeV, the ZZ^* and reducible background for 14.8 fb^{-1} at $\sqrt{s} = 13$ TeV. The estimates are given for the $m_{4\ell}$ mass range 118–129 GeV. Full uncertainties are provided.

Analysis category	Signal				Background		Total expected	Observed
	ggF + $b\bar{b}H$ + $t\bar{t}H$	VBF	WH	ZH	ZZ^*	Z + jets, $t\bar{t}$		
0-jet	11.2 ± 1.4	0.120 ± 0.019	0.047 ± 0.007	0.060 ± 0.006	6.2 ± 0.6	0.84 ± 0.12	18.4 ± 1.6	21
1-jet	5.7 ± 2.4	0.59 ± 0.05	0.137 ± 0.012	0.091 ± 0.008	1.62 ± 0.21	0.44 ± 0.07	8.5 ± 2.4	12
2-jet VBF enriched	1.9 ± 0.9	0.92 ± 0.07	0.074 ± 0.007	0.052 ± 0.005	0.22 ± 0.05	0.24 ± 0.11	3.4 ± 0.9	9
2-jet VH enriched	1.1 ± 0.5	0.084 ± 0.009	0.143 ± 0.012	0.101 ± 0.009	0.166 ± 0.035	0.088 ± 0.011	1.6 ± 0.5	2
VH-leptonic	0.055 ± 0.004	< 0.01	0.067 ± 0.004	0.011 ± 0.001	0.016 ± 0.002	0.012 ± 0.010	0.16 ± 0.01	0
Total	20 ± 4	1.71 ± 0.14	0.47 ± 0.04	0.315 ± 0.027	8.2 ± 0.9	1.62 ± 0.07	32 ± 4	44

